A profile of the final states in $B \to X_s + \gamma$ and an estimate of the branching ratio $BR(B \to K^* + \gamma)$

A. Ali and C. Greub

Deutsches Elektronen Synchrotron DESY, W-2000 Hamburg, FRG

Received 11 January 1991; revised manuscript received 7 February 1991

We present an estimate of the inclusive photon energy- and hadron mass-spectrum in rare B decays $B \to X_s + \gamma$, based on perturbative QCD and a phenomenological model for the B-meson wave function (here X_s denotes hadrons with total strangeness quantum number $S = -1$). The shapes of the spectra are sensitive to the details of the wave function and the top quark mass, m_t, but the normalization is essentially determined by m_t. We find $BR(B \to X_s + \gamma) = (3\text{–}4) \times 10^{-4}$ for $100 \leq m_t \leq 200$ GeV. With the additional assumption that the K* resonance saturates the recoil hadron mass spectrum in the interval $(M_K + M_\pi) \leq m_{X_s} \leq 1$ GeV, we calculate the branching ratio $BR(B \to K^* + \gamma)$ and predict $BR(B \to K^* + \gamma) = (5^{+3}_{-2}) \times 10^{-5}$, where the errors reflect the uncertainties on the hadronic wave function and the top quark mass in the stated range.

1. Introduction

Rare B decays provide potentially fertile grounds for testing the standard model in flavour changing neutral current processes. In this context, radiative decay of the b-quark, $b \to s + \gamma$, has received special attention [1–8]. The present consensus is that QCD effects enhance the decay rate very significantly, resulting in an inclusive branching ratio $BR(b \to s + \gamma) = (3\text{–}4) \times 10^{-4}$, for the top quark mass in the range 100–200 GeV. Apart from fixing the inclusive rate, the calculations for $b \to s + \gamma$ are of little direct help for experimental searches, which so far have been limited to specific final states. The present best experimental upper limit on rare radiative b-decays in an exclusive mode is: $BR(B \to K^* + \gamma) \leq 2.8 \times 10^{-4}$ (90% CL) [9]. Theoretical estimates for $B \to K^* + \gamma$ abound in the literature; the predictions in this case are however dispersed over an order of magnitude [4,10–12]. To make a meaningful comparison of theory and experiment in this sector, it is important to measure the decay rate for $B \to X_s + \gamma$ inclusively, for example via the inclusive photon energy spectrum, as has been advocated by us in ref. [13] (here X_s denotes hadrons with total strangeness $S = -1$). Equivalently, one should devise methods to either reliably calculate the exclusive rates or at least partially constrain theoretical models for rare B-decays from available data on (the not so rare) B- and D-decays. The aim of this paper is to provide a trustworthy profile of the inclusive photon energy and the invariant hadron mass distributions in the decays $B \to X_s + \gamma$.

Our starting point is the recent calculation of the inclusive photon energy spectrum in the rare b-quark decays $b(\bar{q}) \to \gamma + X_s$, which was obtained in perturbative QCD and involved the decays $b \to s + \gamma$ and $b \to s + g + \gamma$ [13]. The Feynman diagrams are shown in fig. 1. We improve upon this calculation in two respects. First, we derive a photon energy spectrum which is better-behaved near the end-point, $E_\gamma \simeq E_\gamma^{\max}$. This is achieved by exponentiating the leading contribution to the photon energy spectrum for large E_γ, which is the region of experimental interest. With the improved spectrum, QCD perturbation theory results can be extended to the region $E_\gamma \simeq E_\gamma^{\max}$. The second improvement is that we strive to implement the B-meson wave function effects on the photon energy and the invariant mass distributions of the hadrons (recoiling against the photon). This is a model dependent enterprise but has its close equivalents in studies of the semileptonic B- and D-decays, where

0370-2693/91/$ 03.50

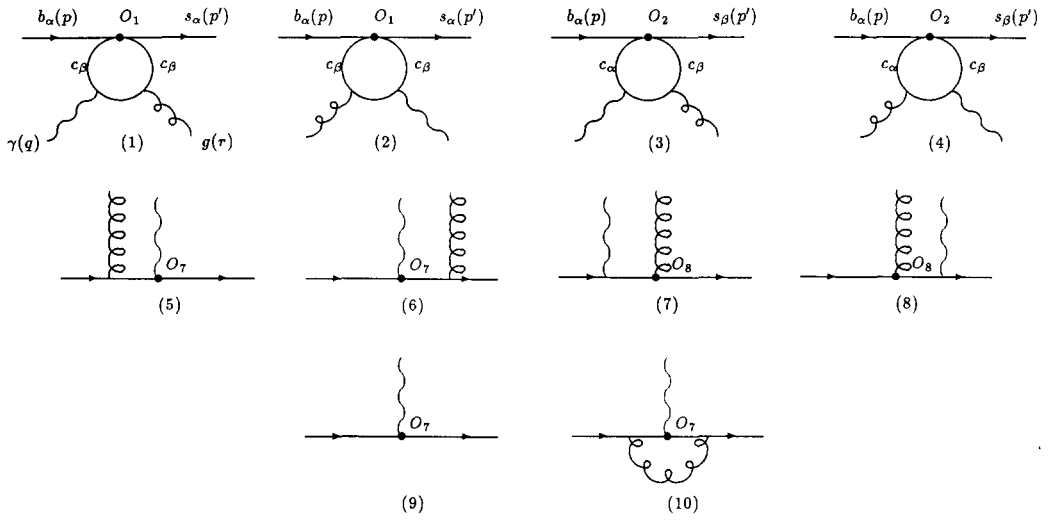

Fig. 1. The Feynman diagrams contributing to the decays b→s+γ and b→s+g+γ.

such non-perturbative effects were modelled to calculate the lepton energy spectra in perturbative QCD [14,15]. We have used recent analyses of the data on semileptonic decays of the B-mesons [16–18] to constrain the B-meson wave function. The resulting distributions $d\Gamma/dE_\gamma$ and $d\Gamma/dM_{X_s}$ for the rare B-decays $B\to X_s+\gamma$ are presented here. Having obtained the invariant mass distribution of the recoil hadrons in the decays $B\to X_s+\gamma$, we integrate this distribution in the interval $(M_K+M_\pi)\leqslant m_{X_s}\leqslant 1$ GeV to estimate the branching ratio for $B\to K^*+\gamma$. This last step appears to us rather sound as it is strongly suggested by the analysis of the (analogous) semileptonic decays of the D-meson in $D\to K+\pi+\ell+\nu_\ell$, where it has been experimentally ascertained that the hadronic mass, recoiling against the $\ell\nu_\ell$-pair in the stated region of kinematic interest, is completely saturated by the K* pole [19]. This enables us to make a prediction for the branching ratio of interest, and we find: $BR(B\to K^*+\gamma)=(5^{+3}_{-2})\times 10^{-5}$, where the central value corresponds to $m_t=140$ GeV and the best fit of the B-meson wave function parametrization from the CLEO data [16], and the errors reflect the uncertainties due to the wave function and the top quark mass in the range $m_t=100$–200 GeV.

2. Photon energy spectrum for $B\to X_s+\gamma$

We briefly discuss a derivation of the inclusive photon energy spectrum for the decays $B\to X_s+\gamma$ in the context of $O(\alpha_s)$ perturbative QCD calculations, including the exponentiation of the E_γ-spectrum in the region $E_\gamma\to E_\gamma^{max}$. The calculations have been done within the framework of an effective hamiltonian [20]. The operator basis for the effective hamiltonian, responsible for the decay under consideration, consists of four-quark operators and the magnetic moment type operators of dimension six. Operators of higher dimension are suppressed by powers of the masses of the heavy particles (W-boson and top quark) which have been integrated out, and hence are not considered here. To leading order in the small (weak)-mixing angles, a complete set of operators relevant for the processes b→sγ, sγg is contained in the effective hamiltonian

$$H_{\rm eff}=-\frac{4G_F}{\sqrt{2}}\lambda_t\sum_{j=1}^{8}C_j(\mu)O_j(\mu)\,, \tag{1}$$

where G_F is the Fermi coupling constant and (V_{ij} are the CKM matrix elements)

$\lambda_t = V_{tb}V_{ts}^*$, $C_j(\mu)$ = Wilson coefficients at scale μ.

The complete set of operators O_j for $B \to X_s + \gamma$ and the coefficient functions $C_j(\mu)$ can be seen in ref. [13], where we have shown that the dominant contributions arise from the operators O_2 and O_7, given below:

$$O_2 = (\bar{c}_{L\alpha}\gamma^\mu b_{L\alpha})(\bar{s}_{L\beta}\gamma_\mu c_{L\beta}), \quad O_7 = (e/16\pi^2)\bar{s}_\alpha \sigma^{\mu\nu}(m_b R + m_s L) b_\alpha F_{\mu\nu},$$

$$L = \tfrac{1}{2}(1-\gamma_5), \quad R = \tfrac{1}{2}(1+\gamma_5), \tag{2}$$

here e denotes the QED coupling constant. The effects of QCD corrections, contained in the Wilson coefficients $C_j(\mu)$, have been evaluated to leading logarithmic accuracy. The coefficients $C_2(\mu)$, $C_7(\mu)$ are given in refs. [20,21]. At $\mu = m_b$, which is the relevant scale for the b quark decay, these coefficients read as follows:

$$C_2(m_b) = \tfrac{1}{2}(\eta^{-6/23} + \eta^{12/23}) C_2(m_W),$$

$$C_7(m_b) = \eta^{-16/23}[C_7(m_W) - \tfrac{58}{135}(\eta^{10/23}-1)C_2(m_W) - \tfrac{29}{189}(\eta^{28/23}-1)C_2(m_W)], \tag{3}$$

with $\eta = \alpha_s(m_b)/\alpha_s(m_W)$. At the scale $\mu = m_W$, where the matching conditions are imposed [22], we have (again to leading logarithmic accuracy)

$$C_2(m_W) = 1, \quad C_7(m_W) = \frac{x}{24(x-1)^4}[6x(3x-2)\log x - (x-1)(8x^2+5x-7)], \tag{4}$$

with $x = m_t^2/m_W^2$.

We recall here that the photon energy spectrum in $b \to s\gamma g$ has a nonintegrable infrared singularity for $E_\gamma \to E_\gamma^{max}$. Adding the process $b \to s\gamma$ with its virtual corrections, the divergences cancel in a distribution sense and one gets a finite expression for $d\Gamma/dx_\gamma$ but the end-point spectrum feels the left-over effects of the infrared singularity and hence $d\Gamma/dx_\gamma$ rises very steeply near the end-point, $x_\gamma \simeq 1$; here x_γ is the fractional energy of the photon, $x_\gamma = E_\gamma/E_\gamma^{max}$. The leading behaviour of the spectrum near $x_\gamma \to 1$ can be traced to the quark splitting $s \to s+g$, having the typical Altarelli–Parisi behaviour [23] (see below). This is all too familiar a situation in the calculation of energy spectra of gauge bosons in fixed order perturbation theory; a very close parallel is the perturbative QCD calculation of the transverse momentum distribution of the intermediate $W^\pm$ and Z^0 bosons produced in hadronic collisions [24,25]. The remedy of this is also well known, namely a resummation of the leading (infrared) logarithms, thereby providing a better description of the spectra near the end-point. We isolate analytically the leading terms [in $O(\alpha_s)$] near the end-point of the photon energy spectrum, and exponentiate these terms in the region $x_\gamma \to 1$.

With the scaled photon energy x_γ defined above, we choose to express the photon energy spectrum as a sum of the following partial fractions:

$$\frac{d\Gamma}{dx_\gamma} = \frac{d\Gamma_F}{dx_\gamma} + \frac{d\Gamma_A}{dx_\gamma} + \frac{d\Gamma_B}{dx_\gamma}. \tag{5}$$

The first term on the RHS of eq. (5) contains the square of the matrix element of the operator O_2 and the interference term of O_2 and O_7; it can be written as a one dimensional integral over the gluon energy in the process $b \to s+g+\gamma$ [13]:

$$\frac{d\Gamma_F}{dx_\gamma} = \frac{G_F^2 |\lambda_t|^2 \alpha\alpha_s(1-r)}{1536\pi^5} \int_{E_g^-}^{E_g^+} (\tau_{22} + \tau_{27}) dE_g,$$

$$\tau_{22} = 2Q_u^2 C_2^2(\mu)(qr)^2 |\kappa|^2 [(m_b^2 - m_s^2)^2 - 2(m_s^2 + m_b^2)(qr)],$$

$$\tau_{27} = 32 Q_u C_2(\mu) C_7(\mu)(qr)^2 \,\mathrm{Re}(\kappa)\left(\frac{m_s^2 m_b^2 (qr)}{(pr)(p'r)} - (m_s^2 + m_b^2)\right). \tag{6}$$

The limits of the E_g integration are

$$E_g^- = (1-r)(1-x_\gamma)\frac{m_b}{2}, \quad E_g^+ = \frac{(1-r)(1-x_\gamma)}{1-\xi}\frac{m_b}{2}, \quad r=\left(\frac{m_s}{m_b}\right)^2, \quad \xi = x_\gamma(1-r)\,. \tag{7}$$

q, r, p and p' denote the four-momenta of the photon, gluon, b-quark and the s-quark, respectively, $Q_u=\frac{2}{3}$, and $C_2(\mu)$ and $C_7(\mu)$ are the Wilson coefficients evaluated at the renormalization scale μ. The function κ is defined as

$$\kappa = \frac{4[2G(t)+t]}{(qr)t}\,,$$

where $t=2qr/m_c^2$ and $G(t)$ is defined by the integral

$$G(t) = \int_0^1 \frac{dy}{y}\log[1-ty(1-y)-i\epsilon]\,, \tag{8}$$

which yields

$$G(t) = -2\,\mathrm{atan}^2\left(\sqrt{\frac{t}{4-t}}\right), \quad t<4\,,$$

$$G(t) = -\tfrac{1}{2}\pi^2 + 2\log^2[\tfrac{1}{2}(\sqrt{t}+\sqrt{t-4})] - 2i\pi\log[\tfrac{1}{2}(\sqrt{t}+\sqrt{t-4})], \quad t>4\,. \tag{9}$$

The second and third terms on the RHS of eq. (5) involve the matrix element squared of the operator O_7. The second term is the finite part of the bremsstrahlung spectrum and it can be expressed as

$$\frac{d\Gamma_A}{dx_\gamma} = C_0\frac{\alpha_s}{3\pi}\left(\frac{x_\gamma(2x_\gamma^2-5x_\gamma-1)(1-r)}{1-\xi} - 2(1+x_\gamma)\log(1-\xi) + \frac{(1-r)x_\gamma(1-x_\gamma)(2x_\gamma-1)}{(1-\xi)^2}\right), \tag{10}$$

$$C_0 = (1-r)^3(1+r)\frac{m_b^5}{32\pi^4}\alpha G_F^2|\lambda_t|^2 C_7^2(\mu)\,. \tag{11}$$

It is clear from eq. (10) that this term is not going to yield the leading $[\propto 1/(1-x_\gamma)]$ contribution. The third term $d\Gamma_B/dx_\gamma$ receives the remaining contributions from the bremsstrahlung diagrams. In addition, there is also a term proportional to $\delta(1-x_\gamma)$ in $d\Gamma_B/dx_\gamma$ stemming from the process $b\to s+\gamma$ including virtual corrections. Both these contributions are individually infrared singular but finite in the sum in a distribution sense. The regularized formula for $d\Gamma_B/dx_\gamma$ will be given elsewhere [26]. Here we only give the expression for $x_\gamma \neq 1$, where we have removed the infrared regularization. The result can be shown to be the following:

$$\frac{d\Gamma_B}{dx_\gamma} = C_0\frac{\alpha_s}{3\pi}\frac{x_\gamma}{1-x_\gamma}\left(-4-\frac{4r}{1-\xi}-\frac{4}{\xi}(1+r)\log(1-\xi)\right). \tag{12}$$

This is the leading contribution to the photon energy spectrum, in the region $x_\gamma\to 1$. Setting $m_s=0$ (i.e. $r=0$), one sees that the leading term in the spectrum is proportional to $\log(1-x_\gamma)/(1-x_\gamma)$, which on integration would contribute a $\log^2(1-s_0)$ term, with s_0 defining the range of x_γ-integration ($s_0 \lesssim x_\gamma \lesssim 1$). For the case $m_s\neq 0$, which is what we use in our calculation, this would give rise to a single log, as shown below. In terms of the parameter s_0, the integral of the term $d\Gamma/dx_\gamma$, is

$$\Gamma_B(s_0) \equiv \int_{s_0}^1 dx_\gamma \frac{d\Gamma_B}{dx_\gamma}\,, \tag{13}$$

$$\Gamma_B(s_0) = C_0\left(1-\frac{4\alpha_s}{3\pi}A(s_0)+\frac{\alpha_s}{3\pi}B(s_0)\right)\Theta(1-s_0)\,, \tag{14}$$

$$A(s_0)=2\log(1-s_0)+\frac{1+r}{1-r}\log\eta_0\log(1-s_0)\,,$$

$$B(s_0)=5\log(r)-8\log(1-r)-4s_0+\frac{4}{1-r}\log\eta_0$$

$$+\frac{1+r}{1-r}\left[-8\log r+4\log r\log(1-r)-\tfrac{4}{3}\pi^2+4\,\mathrm{Li}(r/\eta_0)+4\,\mathrm{Li}(r)+2\log^2\eta_0-4\log\eta_0\log(1-r)\right], \qquad (15)$$

$$\eta_0=1-s_0(1-r),\quad \mathrm{Li}(x)=-\int_0^x\frac{\mathrm{d}t}{t}\log(1-t)\,. \qquad (16)$$

Our exponentiation procedure for the photon energy spectrum follows from the expression for $\Gamma_B(s_0)$. We exponentiate the leading log terms, which are defined by the function $A(s_0)$. Since $\mathrm{d}\Gamma_B/\mathrm{d}x_\gamma=-\mathrm{d}\Gamma_B/\mathrm{d}s_0|_{s_0=x_\gamma}$, the exponentiated version follows

$$\frac{\mathrm{d}\Gamma_B}{\mathrm{d}x_\gamma}=\frac{4\alpha_s}{3\pi}C_0\exp\left[-\frac{4\alpha_s}{3\pi}\log(1-x_\gamma)\left(2+\frac{1+r}{1-r}\log(1-\xi)\right)\right]$$

$$\times\left[\frac{2-\xi}{1-\xi}+\frac{1+r}{1-\xi}\log(1-x_\gamma)-\left(1+\frac{\alpha_s}{3\pi}B(x_\gamma)\right)\left(\frac{2}{1-x_\gamma}+\frac{1+r}{1-r}\frac{\log(1-\xi)}{1-x_\gamma}+\frac{(1+r)\log(1-x_\gamma)}{1-\xi}\right)\right], \qquad (17)$$

with $B(x_\gamma)=B(s_0\to x_\gamma)$. It can be easily checked that after integration this term leads to $\Gamma_B(s_0)$. Also, expanding the exponential and keeping terms of $O(\alpha_s)$ it reproduces the term given in eq. (12) above. In the exponentiated form, the photon energy spectrum is given by the sum of eqs. (6), (10) and (17). In numerical estimates we shall use the exponentiated form only in the region above a certain minimum value of x_γ (typically for $x_\gamma\geq 0.725$).

The photon energy spectrum depends on the mass of the top quark, as was shown in ref. [13], in addition to the b- and s-quark masses. We shall use in this section the values $m_b=5.0$ GeV and $m_s=0.5$ GeV, which will be replaced by the physical masses and threshold in the next section, after we have specified our model for the hadronic wave function. In fig. 2 we show the photon energy spectrum, $(1/\Gamma_{tot})\mathrm{d}\Gamma/\mathrm{d}E_\gamma$, for the decay $B\to X_s+\gamma$, assuming $m_t=140$ GeV, for both the non-exponentiated [i.e. $O(\alpha_s)$], and the exponentiated cases. The exponentiated photon energy spectrum for the large E_γ-region shows the characteristic slowing down due to the improved infrared behaviour (only integrable singularity) which increases the domain of applicability of perturbation theory to higher values of E_γ. The exponentiated spectrum is then used as input to incorporate the B-meson wave function effects which we discuss next.

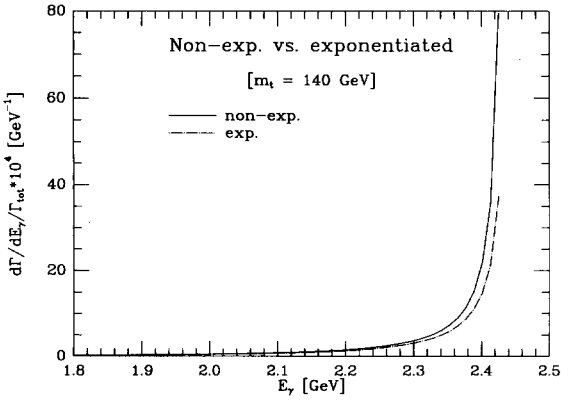

Fig. 2. Inclusive photon energy spectrum for the process $B\to X_s+\gamma$ in perturbative QCD and $m_t=140$ GeV, corresponding to the $O(\alpha\alpha_s)$ contribution to the branching ratio (solid curve), and exponentiated version (dash-dotted curve).

3. B-meson wave function effects

We use a simple model first written in ref. [14], and also employed by Altarelli et al. [15], to implement the D- and B-meson bound state effects on the lepton energy spectra in D- and B-semileptonic decays. With the help of this model, which provides a good description of the lepton energy spectra, we calculate the corresponding wave function effects on the photon energy and hadronic mass spectra in the decays $B\to X_s+\gamma$. In this model the B-quark, whose decays determine the dynamics, is given a non-zero momentum having a gaussian distribution, represented by an a priori free (but adjustable) parameter, p_F:

$$\phi(p)=\frac{4}{\sqrt{\pi}\,p_F^3}\exp\left(\frac{-p^2}{p_F^2}\right),\quad p=|\boldsymbol{p}|\,. \tag{18}$$

The energy–momentum constraint is imposed in the form

$$W^2=M_B^2+m_q^2-2M_B\sqrt{p^2+m_q^2}\,, \tag{19}$$

where M_B is the B-meson mass, W is the effective mass of the b-quark, and m_q is the mass of the spectator quark in the B-meson, $B=b\bar{q}$. The mass of the decaying b-quark varies according to eq. (19). The photon energy spectrum from the decay of the B-meson at rest is then given by

$$\frac{d\Gamma}{dE_\gamma}=\int_0^{p_{max}}\phi(p)p^2dp\,\frac{d\Gamma_b}{dE_\gamma}(W,p,E)\,, \tag{20}$$

where $\phi(p)$ is normalized as

$$\int_0^\infty\phi(p)p^2dp=1\,. \tag{21}$$

p_{max} is the maximum allowed value of p, and $d\Gamma_b/dE$ is the photon energy spectrum from the decay of the b-quark in flight, having a mass W and momentum p. This can be obtained by Lorentz boosting the b-quark decay spectrum at rest. The physical kinematic threshold in the problem, namely $m_X\geq m_K+m_\pi$ and the energy–momentum constraint eq. (19) have to be respected. The constraint from the B-mass is well appreciated by the practitioners of this model, but we would like to emphasize the threshold constraint here. Since we prefer to use a quark mass $m_s=0.5$ GeV in our perturbative calculation, which is lower than the kinematic threshold, one could get contributions to the photon energy spectrum in an unphysical region. We have imposed rigorously the physical threshold, but maintain the normalization of the integrated E_γ-spectrum (i.e., the partial decay width) by an overall (minor) adjustment of the spectrum. The branching ratio for the inclusive decay $B\to\gamma+X_s$,

$$BR(B\to\gamma+X_s)=\frac{\Gamma(B\to\gamma+X_s)}{\Gamma_{tot}}\,, \tag{22}$$

is now calculated using Γ as given in (20), and the inclusive b quark width, Γ_{tot}:

$$\Gamma_{tot}=(r_u|V_{ub}|^2+r_c|V_{cb}|^2)\Gamma_0,\quad \Gamma_0=\frac{W_{eff}^5G_F^2}{192\pi^3},\quad r_u\approx 7,\quad r_c\approx 3\,. \tag{23}$$

The values of r_u and r_c include phase space and QCD corrections [27]. The dependence on the effective b-quark mass, W_{eff}, which enters as the fifth power in both Γ_{tot} and the inclusive width for $B\to X_s+\gamma$, cancels to a very large extent in $BR(B\to X_s+\gamma)$, when calculated using eq. (23). Note that the spectra and the decay rate for $B\to X_s+\gamma$ are calculated directly in terms of the B-meson mass. The effective b-quark mass, entering in Γ_{tot}, can also be expressed in terms of the B-meson mass and the parameter p_F. A very good (numerical) functional dependence of W_{eff} for the present model can be parametrized as

$$W_{\rm eff}^2 \simeq M_B^2 - 2M_B \cdot p_F \cdot 1.13 \,. \tag{24}$$

4. Numerical results

Having specified the perturbative and non-perturbative aspects of our calculations, we proceed to present numerical results for the final states in the decays $B \to X_s + \gamma$, taking into account all the available experimental constraints. There are two important parameters that influence the rates and shapes of the spectra, namely m_t and p_F, since we have traded the b-quark mass for the B-meson mass and p_F. The present bound on the top quark mass coming from the analysis of the electroweak data is $m_t = 140 \pm 40$ GeV [28]. We have varied m_t in the range $100 \leqslant m_t \leqslant 200$ GeV. The parameter p_F has been experimentally constrained to be $0.21 \leqslant p_F \leqslant 0.39$ GeV, from recent analysis of the CLEO data [16], with the numbers from the ARGUS analysis [17] very similar. The dependence on m_s is very mild; however, as emphasized earlier the threshold condition $M_{X_s} \geqslant m_K + m_\pi$ must be maintained. The other parameters used in the numerical estimates are: $m_W = 80.2$ GeV, $G_F = 1.16637 \times 10^{-5}$ GeV^{-2}, $\alpha = 1/137.036$, $\alpha_s = 0.23$ (corresponding to $N_f = 5$ and $\Lambda = 0.15$ GeV), $|V_{ub}| \approx 0.0075$ and $|V_{cb}| = |V_{ts}| \approx 0.045$.

In fig. 3 we show the inclusive photon spectrum in the process $B \to X_s + \gamma$, for the stated range of p_F and $m_t = 140$ GeV. The photon spectrum peaks around $\simeq 2.55$ GeV, though the shape is now dependent on p_F. The dependence of the normalization on p_F is, however, completely negligible, remaining within $\pm 1\%$ for the entire p_F-range. The photon energy spectrum also depends on the top quark mass, as shown in fig. 4. The branching ratio dependence on the top quark mass is, within $\pm 1\%$, the same as calculated in ref. [13] in the context of perturbation theory alone.

The invariant mass distribution of the hadrons recoiling against the photon in the inclusive process $B \to X_s + \gamma$ is shown in fig. 5, for three values of p_F, which bracket the present uncertainty on this parameter [16], and $m_t = 140$ GeV. We remark that the shape of the hadron mass spectra is rather sensitive to p_F, with the peak of the distributions significantly shifted from around $\simeq 1.25$ GeV (for $p_F = 0.21$ GeV) to $\simeq 1.6$ GeV (for $p_F = 0.39$ GeV). For all these cases, the distributions in fig. 5 are fairly broad (with the full width at half maximum $\simeq$ 1

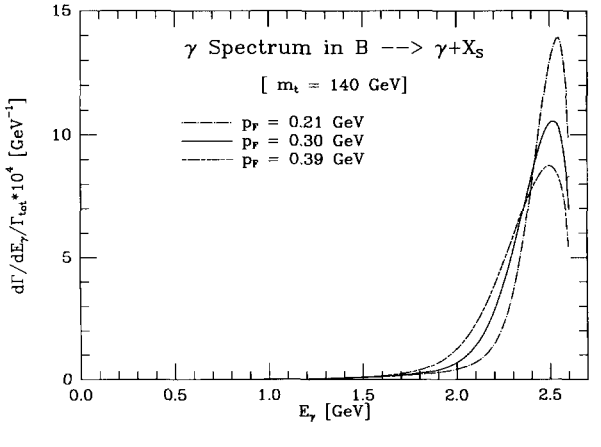

Fig. 3. Inclusive photon energy spectrum for the process $B \to X_s + \gamma$ using perturbative QCD and the B-meson wave function model described in the text, and $m_t = 140$ GeV. The three indicated values of the parameter p_F bracket the recent ($\pm 1\sigma$)-fits of the CLEO data from the lepton energy spectrum in B-decays [16].

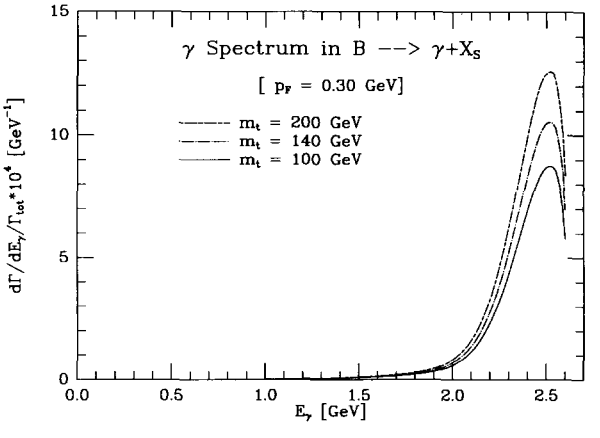

Fig. 4. Inclusive photon energy spectrum for the process $B \to X_s + \gamma$ using perturbative QCD and the B-meson wave function model described in the text, with the parameter p_F set to 0.3 GeV, and three representative values of the top quark mass as indicated.

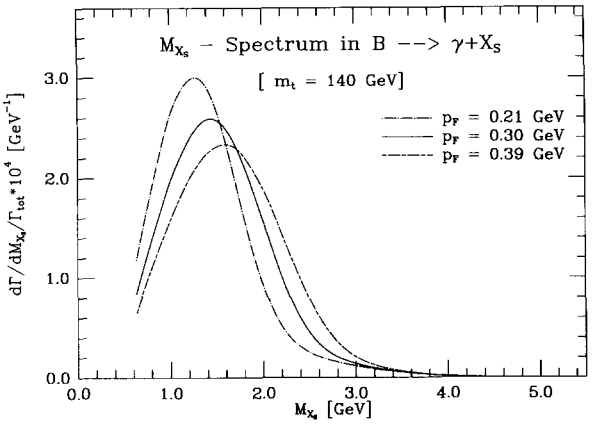

Fig. 5. Invariant mass distribution of the hadrons recoiling against the photon in the decays $B \to X_s + \gamma$, using perturbative QCD, the B-meson wave function model described in the text, and $m_t = 140$ GeV. The three indicated values of the parameter p_F correspond to the recent ($\pm 1\sigma$)-fits of the CLEO data from the lepton energy spectrum in B-decays.

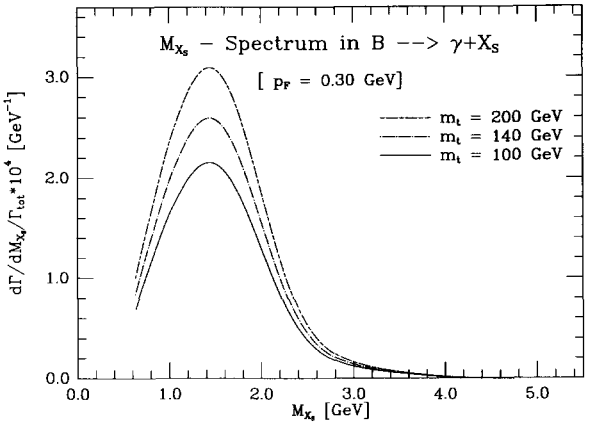

Fig. 6. The same as in fig. 4, but with $p_F = 0.3$ GeV, and three indicated values of the top quark mass.

Table 1
Branching ratio for the decay $B \to K^* + \gamma$ [$\times 10^{-5}$] for the indicated values of the top quark mass, and the parameter p_F as determined in semileptonic β-decays (see text).

m_t [GeV]	BR($B \to K^* + \gamma$) [$\times 10^{-5}$]		
	$p_F = 0.21$ GeV	$p_F = 0.30$ GeV	$p_F = 0.39$ GeV
100	5.8	4.2	3.3
140	6.9	5.0	4.0
200	8.3	6.0	4.8

GeV), which we interpret as a statement that the inclusive decays $B \to X_s + \gamma$ are dominated by multibody final states, involving a kaon and a multitude of pions, with no single resonance dominating. The dependence of the invariant mass distribution of the hadrons on the top quark mass is shown in fig. 6.

Finally, having a profile of the invariant mass distribution of the recoiling hadrons in $B \to X_s + \gamma$, we integrate this spectrum in the range $(m_K + m_\pi) \leq m_{X_s} \leq 1.0$ GeV to estimate the branching ratio for $B \to K^* + \gamma$. As stated in the introduction, this procedure is suggested by the hadron spectrum in the semileptonic D-decays, which in the stated range is completely saturated by the K*-resonance. The resulting branching ratio $B \to K^* + \gamma$ is given in table 1, for the indicated range of m_t and p_F. Taking the central entry in table 1 ($m_t = 140$ GeV, $p_F = 0.3$ GeV), we estimate $B \to K^* + \gamma \simeq 5 \times 10^{-5}$. This is approximately a factor 5 smaller than the present experimental bound [9].

Acknowledgement

We would like to thank Sheldon Stone for communication of the recent analysis of CLEO data on B-meson

semileptonic decays. We also thank Ed. Thorndike for a correspondence and Thomas Mannel and Paul Söding for discussions.

References

[1] M.A. Shifman, A.I. Vainshtein and V.I. Zakharov, Phys. Rev. D 18 (1978) 2583.
[2] B.A. Campbell and P.J. O'Donnell, Phys. Rev. D 25 (1982) 1989.
[3] S. Bertolini, F. Borzumati and A. Masiero, Phys. Rev. Lett. 59 (1987) 180.
[4] N.G. Deshpande et al., Phys. Rev. Lett. 59 (1987) 183.
[5] B. Grinstein, R. Springer and M.B. Wise, Phys. Lett. B 202 (1988) 138.
[6] D. Cocolicchio et al., in: Proc. Conf. Italian Physical Society, Vol. 9, eds. E. De Sanctis, M. Greco, M. Piccolo and S. Tazzari (1988).
[7] R. Grigjanis et al., Phys. Lett. B 213 (1988) 355; University of Toronto report UTPT-89-21 (1989).
[8] M. Sutherland, in: Proc. Workshop on $B\bar{B}$ factories and related physics issues (Blois, France, June–July 1989).
[9] Particle Data group, J.J. Hernández et al., Review of particle properties, Phys. Lett. B 239 (1990) 1.
[10] T. Altomari, Phys. Rev. D 37 (1988) 677.
[11] C.A. Dominguez, N. Paver and Riazuddin, Phys. Lett. B 214 (1988) 459.
[12] P.J. O'Donnel, in: Quarks, gluons and hadronic matter, eds., R. Viollier and N. Warner (World Scientific, Singapore, 1987); Phys. Lett. B 175 (1986) 369.
[13] A. Ali and C. Greub, DESY report 90-102 (1990), Z. Phys. C., to be published.
[14] A. Ali and E. Pietarinen, Nucl. Phys. B 154 (1979) 519.
[15] G. Altarelli et al., Nucl. Phys. B 208 (1982) 365.
[16] CLEO Collab., R. Fulton et al., Phys. Rev. Lett. 64 (1990) 16;
S. Stone, private communication.
[17] ARGUS Collab., H. Albrecht et al., Phys. Lett. B 234 (1990) 409; DESY report DESY 90-088 (1990).
[18] Crystal Ball Collab., K. Wachs et al., Z. Phys. C 42 (1989) 33.
[19] E691 Collab., J.C. Anjos et al., Phys. Rev. Lett. 62 (1989) 1587.
[20] B. Grinstein, R. Springer and M.B. Wise, Caltech preprint CALT-68-1574, Harvard preprint HUTP-89/A048 (1989).
[21] B. Grinstein, M.J. Savage and M.B. Wise, Nucl. Phys. B 319 (1989) 271.
[22] T. Inami and C.S. Lim, Progr. Theor. Phys. 65 (1981) 297.
[23] V.N. Gribov and L.N. Lipatov, Sov. J. Nucl. Phys. 15 (1972) 78;
G. Altarelli and G. Parisi, Nucl. Phys. B 126 (1977) 298.
[24] J.M. Bettems, C. Greub and P. Minkowski, University of Bern preprint BUTP-90/13 (1990).
[25] G. Altarelli, R.K. Ellis, M. Greco and G. Martinelli, Nucl. Phys. B 246 (1984) 12.
[26] A. Ali and C. Greub, DESY report, in preparation.
[27] A. Paschos and U. Türke, Phys. Rep. 178 (1989) 145.
[28] F. Dydak, Talk presented at XXV Intern. Conf. on High energy physics (Singapore, August 1990);
D. Haidt, in: EPS Conf. on High energy physics '89 (Madrid, Spain, 1989), eds. F. Barreiro et al., Nucl. Phys. B (Proc. Suppl.) 16 (1990) 294;
J. Ellis and G.L. Fogli, CERN report CERN-TH-5817 (1990);
P. Langacker, Phys. Rev. Lett. 63 (1989) 1920.